Journal of Solid State Chemistry **150,** 330–335 (2000)
doi:10.1006/jssc.1999.8598, available online at http://www.idealibrary.com on IDEAL®

Hydrothermal Synthesis and Crystal Structure of a New Barium Vanadium Bronze $Ba_{1+x}V_8O_{21}$ with a Tunnel Structure

Yoshio Oka,*,[1] Takeshi Yao,† and Naoichi Yamamoto‡

*Department of Natural Environment Sciences, Faculty of Integrated Human Studies, Kyoto University, Kyoto 606-8501, Japan;
†Department of Fundamental Energy Sciences, Graduate School of Energy Sciences, Kyoto University, Kyoto 606-8501, Japan; and
‡Graduate School of Human and Environmental Studies, Kyoto University, Kyoto 606-8501, Japan

Received September 30, 1999; in revised form November 11, 1999; accepted December 4, 1999

A barium vanadium bronze $Ba_{1+x}V_8O_{21}$ has been hydrothermally synthesized and structurally characterized. Hydrothermal treatment of a suspension of VO_2 powders in $Ba(NO_3)_2$ solution at 350°C yielded a fibrous brown compound having non-stoichiometric composition $Ba_{1+x}V_8O_{21}$ ($x = 0.13$). Single-crystal X-ray diffractometry revealed the monoclinic system $C2/m$ with $a = 15.144(6)$, $b = 3.596(4)$, $c = 14.972(3)$ Å, $\beta = 90.08(3)°$, and $Z = 2$, with the refinement based on 2021 reflections with $I > 3\sigma(I)$ converged to $R = 0.054$ and $R_w = 0.046$. A new tunnel-type bronze structure was disclosed in which VO_6 octahedra and VO_5 trigonal bipyramids form a V–O framework with a tunnel cavity running along [010]. The Ba atom partially occupies the tunnel site with more than half occupancy of 56.6%, which causes displacement of the Ba atom and further displacement of V and O atoms along the tunnel axis. $Ba_{1+x}V_8O_{21}$ is the first tunnel-type barium vanadium bronze whose structure has been fully determined.

INTRODUCTION

Barium vanadium oxides with V^{IV}/V^{V} mixed valences are often classified into vanadium bronze compounds denoted by barium vanadium bronze. Vanadium bronzes adopt V–O framework structures of layered or tunnel types, where foreign metal ions and water molecules are incorporated in interstitial spaces. There are a variety of V–O framework structures, which are mostly layered types such as α, δ, γ, and σ phases and tunnel types such as β phase. Their structural features make vanadium bronzes promising materials for advanced technologies such as secondary lithium batteries and catalysts (1). Recently, vanadium bronzes attract much attention due to their low-dimensional magnetic properties arising from V^{4+} ions with $S = 1/2$ spins (2).

There are several barium vanadium bronzes most of which exhibit their own V–O framework structures of crystallographic interest. For example, layered types are found in BaV_3O_8 (3), $BaV_6O_{16} \cdot nH_2O$ (4), and $BaV_7O_{16} \cdot nH_2O$ (5) of which BaV_3O_8 and $BaV_7O_{16} \cdot nH_2O$ adopt their own layer-type structures and $BaV_6O_{16} \cdot nH_2O$ adopts a layer structure similar to that of γ-$Li_{1+x}V_3O_8$ (6). More interestingly, $Ba_{0.4}V_3O_8(VO)_{0.4} \cdot nH_2O$ adopts an intermediate type between layered and tunnel type: namely, V_3O_8 layers are partially bridged by VO_5 trigonal bipyramids (7). Bouloux *et al.* studied the $BaO–VO_2–V_2O_5$ phase diagram and reported layered-type α-$Ba_xV_2O_5$ (α phase) and tunnel-type β–$Ba_{0.17}V_2O_5$ (β phase) but their crystallographic details have not been given (8). They also reported $Ba_{0.40}V_7O_{16}$ in the diagram that seems to be a member of barium vanadium bronzes although its structure remains unknown (8). Another bronze-like compound BaV_8O_{21-x} is seen in the diagram that was first reported by Fotiev *et al.* (9) but only its powder X-ray pattern is known.

New members of the barium vanadium bronze family may be disclosed by employing synthetic methods other than solid-state reactions. One such method is a hydrothermal synthesis, which also has a great advantage of growing single crystals suitable for structure determination. Actually, some barium vanadium bronzes have been hydrothermally synthesized and their structures have been solved using single crystals (3–6). In the present study, hydrothermal synthesis was successfully applied to produce a new barium vanadium bronze with a tunnel-type structure.

EXPERIMENTAL

Sample Preparation

Starting materials for the hydrothermal synthesis are $VO_2(A)$ powders and $Ba(NO_3)_2$ solutions; $VO_2(A)$ powders were prepared hydrothermally from $VO(OH)_2$ powders as described elsewhere (10). A suspension of 400 mg $VO_2(A)$ powders in 50 ml 0.05 M $Ba(NO_3)_2$ solution was sealed in

[1] To whom correspondence should be addressed. E-mail: oka@kagaku.h.kyoto-u.ac.jp.

0022-4596/00 $35.00

a quartz ampule followed by hydrothermal treatment in an autoclave at 350°C for 40 h. A brown fibrous product was separated by filtration: columnar crystals of BaV_2O_6 (10) were sometimes included and easily removed by picking out from the product. A crystalline phase of the brown fiber could not be identified by powder X-ray diffraction. Chemical analysis, thermogravimetry (TG), and energy dispersive X-ray analysis (EDX) gave a non-stoichiometric composition $Ba_{1+x}V_8O_{21}$ with $x = 0.12(2)$. Single crystals of the brown fiber with a flat rod shape were grown in the product and collected under an optical microscope.

Single-Crystal X-Ray Diffraction

Single crystals of the brown fiber gave somewhat elongated diffraction peaks, and a crystal suitable for structure determination was selected with effort by Weissenberg camera work. The crystal with a size of $0.35 \times 0.05 \times 0.01$ mm was mounted on a Rigaku AFC-7R X-ray diffractometer equipped with monochromatized Mo$K\alpha$ radiation. Data collection was made using the 2θ–ω step scanning method with a step width of $\Delta\omega = (0.89 + 0.30 \tan\theta)^\circ$ up to $2\theta = 80^\circ$, where no significant intensity fluctuation was observed by monitoring three standard reflections every 150 data. A total of 3823 reflections were collected, of which 2021 reflections with $I > 3\sigma(I)$ were used in the structure refinements. An empirical absorption correction based on the ψ scan method was applied resulting in transmission factors 0.695–0.863. All of the calculations for data processing and structure determination were carried out using SDP for Windows (12) and teXsan for Windows (13) software.

The monoclinic system was detected with unit cell parameters of $a = 15.144(6)$, $b = 3.596(4)$, $c = 14.972(3)$ Å, $\beta = 90.08(3)^\circ$ determined from 20 reflections in a 2θ range of $25.3^\circ < 2\theta < 29.9^\circ$. The formula unit number is certainly $Z = 2$ corresponding to a proper value of 3.587 g cm^{-3} for the calculated density. Possible space groups were $C2/m$, Cm, and $C2$, of which $C2/m$ was chosen since the intensity statistics strongly suggested the centrosymmetric option. The structure was solved by the direct method and subsequent differential Fourier analysis using the software provided by SDP for Windows (12). Positions of four V atoms were first located and then one Ba position, which had to be partially filled. Oxygen positions were found successively in differential Fourier maps. Final least-squares refinements carried out using teXsan for Windows (13) converged to $R = 0.056$ and $R_w = 0.046$. Full occupancies for the V sites were confirmed. Occupancy of the Ba site was refined to 0.564(2), which gives the composition $Ba_{1+x}V_8O_{21}$ with $x = 0.128(4)$, which is in good agreement with $x = 0.12(2)$ obtained by chemical analysis. Experimental and crystallographic parameters are listed in Table 1, atomic coordinates and equivalent temperature factors are given in Table 2, and anisotropic displacement parameters are presented in Table 3.

TABLE 1
Experimental and Crystallographic Parameters of $Ba_{1+x}V_8O_{21}$

Chemical Formula	$Ba_{1.13}V_8O_{21}$
Space group	$C2/m$
a (Å)	15.144(6)
b (Å)	3.596(4)
c (Å)	14.972(3)
β (°)	90.08(3)
V (Å^3)	815.4(7)
Z	2
D_c (g cm^{-3})	3.587
μ (Mo$K\alpha$) (cm^{-1})	71.59
Number of reflections ($I > 0$)	3725
Number of reflections ($I > 3\sigma(I)$)	2021
R_{int}	0.034
Number of variables	96
R/R_w	0.054/0.046
$\Delta\rho_{max/min}$ (e/Å^3)	1.56/−1.73

RESULTS AND DISCUSSION

Description of Crystal Structure

Figure 1 depicts the crystal structure of $Ba_{1+x}V_8O_{21}$ viewed along [010]. The structure consists of V(1)O_6, V(3)O_6, and V(4)O_6 octahedra and V(2)O_5 trigonal bipyramids for which V–O bond distances and O–V–O bond

TABLE 2
Atomic Coordinates and Equivalent Temperature Factors of $Ba_{1+x}V_8O_{21}$

Atom	x	y	z	B_{eq} (Å^2)
Ba[a]	0.52201(4)	0	0.31197(4)	2.309(13)
V(1)	0.90703(5)	0	0.07149(5)	0.708(10)
V(2)	0.82947(5)	0	0.47561(5)	0.763(10)
V(3)	0.68682(5)	0	0.06955(4)	0.580(9)
V(4)	0.80658(6)	0	0.26670(5)	1.600(15)
O(1)	0	0	0	1.14(7)
O(2)	0.38307(19)	0	0.04851(19)	0.75(4)
O(3)	0.19425(19)	0	0.03320(19)	0.71(4)
O(4)	0.78319(19)	0	0.14016(19)	0.88(5)
O(5)	0.6090(2)	0	0.1413(2)	1.26(6)
O(6)	0.8820(2)	0	0.37310(19)	1.03(5)
O(7)	0.3363(3)	0	0.2580(2)	1.33(6)
O(8)	0.9511(2)	0	0.1730(2)	1.30(6)
O(9)	0.2904(2)	0	0.4713(2)	1.35(6)
O(10)	0.0943(3)	0	0.4503(3)	2.59(9)
O(11)	0.7099(3)	0	0.3099(3)	2.48(9)

[a] Site occupancy = 0.564(2).

TABLE 3
Anisotropic Displacement Parameters (Å^2) of $Ba_{1+x}V_8O_{21}$[a]

Atom	U_{11}	U_{22}	U_{33}	U_{13}
Ba	0.0158(2)	0.0565(5)	0.0154(2)	−0.00120(17)
V(1)	0.0127(3)	0.0048(2)	0.0094(3)	−0.0021(2)
V(2)	0.0126(3)	0.0064(3)	0.0099(3)	0.0024(2)
V(3)	0.0088(2)	0.0047(2)	0.0085(2)	0.00039(18)
V(4)	0.0119(3)	0.0397(6)	0.0092(3)	0.0001(2)
O(1)	0.0102(17)	0.0118(19)	0.021(2)	0.0097(15)
O(2)	0.0116(12)	0.0067(11)	0.0102(11)	−0.0001(9)
O(3)	0.0106(12)	0.0050(10)	0.0116(11)	0.0008(9)
O(4)	0.0105(12)	0.0131(13)	0.0100(11)	−0.0026(9)
O(5)	0.0156(14)	0.0166(15)	0.0157(14)	0.0049(11)
O(6)	0.0166(14)	0.0163(14)	0.0063(10)	0.0028(9)
O(7)	0.0296(19)	0.0095(13)	0.0116(13)	−0.0012(12)
O(8)	0.0197(16)	0.0173(16)	0.0124(13)	−0.0036(11)
O(9)	0.0232(17)	0.0078(13)	0.0203(15)	0.0110(13)
O(10)	0.0197(18)	0.062(3)	0.0167(16)	−0.0024(13)
O(11)	0.0218(19)	0.055(3)	0.0176(17)	0.0048(14)

[a] $U_{12} = U_{23} = 0$.

angles are given in Table 4 and ORTEP drawings are shown in Fig. 2. Edge-sharing $V(1)O_6$–$V(3)O_6$ units are piled up along [010] to form an edge-sharing zig-zag column that is a common structure unit in vanadium bronzes. $V(4)O_6$ octahedra are attached to the column by sharing O(4)–O(8) edges with $V(1)O_6$ octahedra to form a V–O octahedral column along [010]. $V(2)O_5$ trigonal bipyramids form an edge-sharing zig-zag chain along [010] that is again a common structure unit in vanadium bronzes. The octahedral columns and the zig-zag chains are connected alternately by sharing O(6) vertices forming a V_8O_{22} layer in (100). The layers are linked by sharing O(1) vertices of $V(1)O_6$ octahedra to form a V_8O_{21} framework having a tunnel space running along [010]. The tunnel-type framework structure of $Ba_{1+x}V_8O_{21}$ is thus constructed.

The Ba atom resides on the tunnel site with 56.4% occupancy and is coordinated by nine oxygens as depicted in Fig. 3 to form a BaO_9 polyhedron for which Ba–O bond distances are listed in Table 5. The half occupancy of the Ba site gives the stoichiometric composition BaV_8O_{21}, where the Ba atom would occupy every other site along [010] to minimize the Ba^{2+}–Ba^{2+} repulsion. In the case of 56.4% occupancy, about one quarter of the Ba atom should have neighboring Ba atoms 3.6 Å apart along [010], which must further separate neighboring Ba atoms due to the Ba^{2+}–Ba^{2+} repulsion. Consequently, the Ba atom more or less displaces along [010] as seen in the relatively high U_{22} value of the Ba atom in Table 3. As seen in Fig. 3, the BaO_9 polyhedron consists of O(5), O(7), and O(11) at $y = 0$ and O(6), O(8), and O(10) at $y = -0.5$ and 0.5 of which O(11) and O(10) exhibit larger U_{22} values (Table 3). Figure 4 shows the scheme of Ba–O(11)–V(4) and Ba–O(10)–V(2) bonding. It is normal that O(11), with the shortest Ba–O distance (2.845 Å), displaces by the influence of the Ba atom. The displacement of O(11) further causes the displacement of V(4) through the short V(4)–O(11) bond (1.601 Å) as seen in Fig. 4. It is, however, strange that O(10) with a longer Ba–O distance (2.952 Å) displaces just like O(11), while O(5), O(6), O(7), and O(8) with Ba–O distances of 2.877–2.951 Å exhibit no appreciable displacements along [010]. This may be because O(10) is an apical oxygen of the $V(2)O_5$ trigonal bipyramid bonding solely to V(2) in the V–O framework. In spite of the large displacement of O(10), V(2) shows no appreciable displacement along [010] different from the case of O(11) and V(4) (see Table 3 and Fig. 4). It is speculated in Fig. 4 that neighboring V(4)–V(4) are linked along [010] by sharing O(7) vertices while neighboring

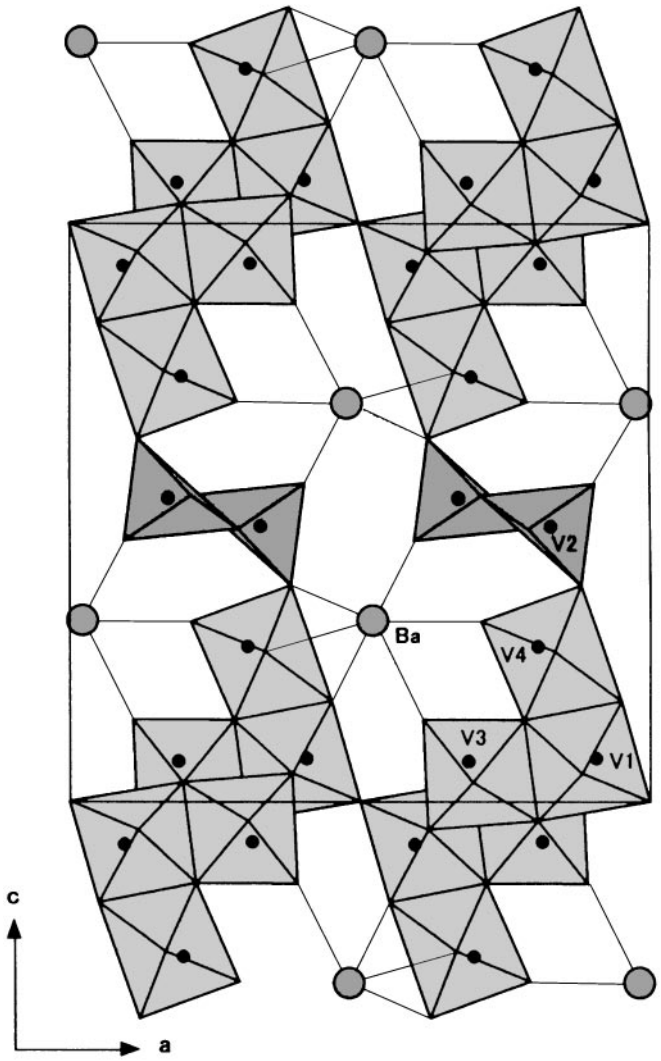

FIG. 1. Crystal structure of $Ba_{1+x}V_8O_{21}$ viewed along [010].

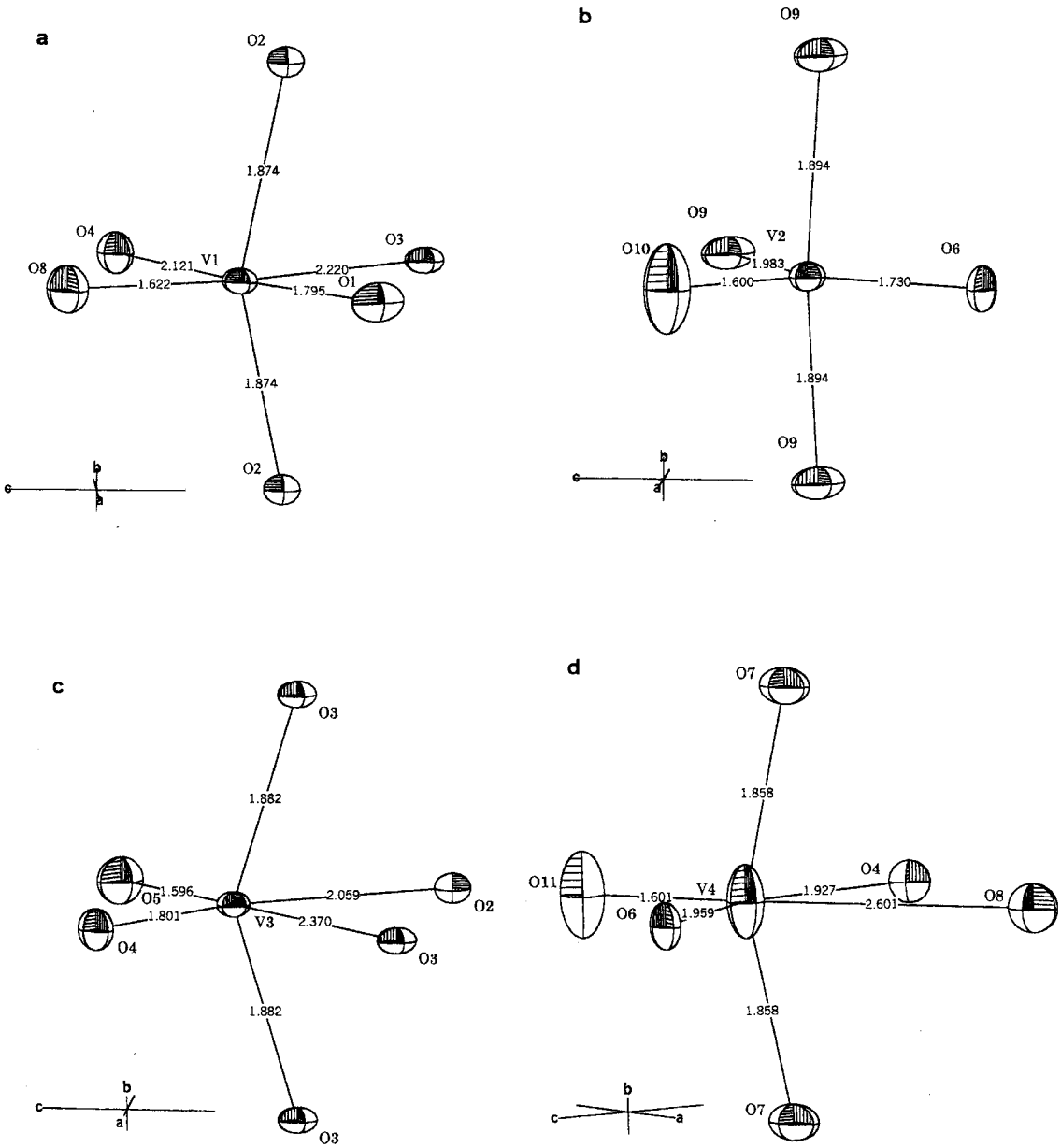

FIG. 2. ORTEP drawings for V–O polyhedra with 50% probability: (a) $V(1)O_6$ octahedron, (b) $V(2)O_5$ trigonal bipyramid, (c) $V(3)O_6$ octahedron, and (d) $V(4)O_6$ octahedron.

V(2)–V(2) by sharing O(9)–O(9) edges, which may make V(4) more displaceable than V(2).

$Ba_{1+x}V_8O_{21}$ exhibits a mixed-valence state V^{IV}/V^{V} with average oxidation number of 4.97. Bond valence calculations were made using equations by Brown and Wu (14) and by Waltersson (15) for comparison and the results are given in Table 6. It is said that V(2) and V(3) are certainly V^{V} and that V(1) is probably V^{V}. Therefore, V(4) must be of mixed valence with an estimated oxidation number of 4.88, or one eighth of V(4) is V^{IV}.

Hydrothermal Synthesis of $Ba_{1+x}V_8O_{21}$

The present hydrothermal system of $Ba(NO_3)_2$–VO_2 (or $VO(OH)_2$) yields mainly hewettite-like $Ba_{1+x}V_6O_{16}\cdot nH_2O$ ($x \approx 0.2$) with mixed-valence V^{IV}/V^{V} classified into barium vanadium bronzes; when VO_2 is substituted for V_2O_5, another hewettite-like $BaV_6O_{16}\cdot nH_2O$ with no V^{IV} is produced (4). The hewettite-like $Ba_{1+x}V_6O_{16}\cdot nH_2O$ is formed at reaction temperatures below 300°C. The brown-fibrous product of $Ba_{1+x}V_8O_{21}$ appears with rising reaction

TABLE 4
V–O Bond Distances (Å) and O–V–O Bond Angles (°) for V–O Polyhedra

$V(1)O_6$ octahedron					
V(1)–O(1)^{i}	1.795(1)	V(1)–O(2)^{ii,iii}	1.874(2)	V(1)–O(3)^{iv}	2.221(4)
V(1)–O(4)	2.121(4)	V(1)–O(8)	1.622(4)		
O(1)^{i}–V(1)–O(2)^{ii,iii}	91.4(1)	O(1)^{i}–V(1)–O(3)^{iv}	95.4(1)		
O(1)^{i}–V(1)–O(4)	169.5(1)	O(1)^{i}–V(1)–O(8)	104.0(2)		
O(2)^{ii}–V(1)–O(2)^{iii}	147.2(2)	O(2)^{ii,iii}–V(1)–O(3)^{iv}	73.6(1)		
O(2)^{ii,iii}–V(1)–O(4)	85.7(1)	O(2)^{ii,iii}–V(1)–O(8)	105.5(1)		
O(3)^{iv}–V(1)–O(4)	74.2(1)	O(3)^{iv}–V(1)–O(8)	160.6(2)		
O(4)–V(1)–O(8)	86.5(2)				
$V(2)O_5$ trigonal bipyramid					
V(2)–O(6)	1.730(4)	V(2)–O(9)^{ii,iii}	1.894(2)	V(2)–O(9)^{iv}	1.983(5)
V(2)–O(10)^{iv}	1.600(5)				
O(6)–V(2)–O(9)^{ii,iii}	96.5(1)	O(6)–V(2)–O(9)^{iv}	141.1(2)		
O(6)–V(2)–O(10)^{iv}	106.4(2)	O(9)^{ii}–V(2)–O(9)^{iii}	143.4(3)		
O(9)^{ii,iii}–V(2)–O(9)^{iv}	74.2(1)	O(9)^{ii,iii}–V(2)–O(10)^{iv}	104.4(2)		
O(9)^{iv}–V(2)–O(10)^{iv}	112.5(2)				
$V(3)O_6$ octahedron					
V(3)–O(2)^{iv}	2.059(4)	V(3)–O(3)^{ii,iii}	1.882(2)	V(3)–O(3)^{iv}	2.370(4)
V(3)–O(4)	1.801(4)	V(3)–O(5)	1.596(4)		
O(2)^{iv}–V(3)–O(3)^{ii,iii}	77.4(1)	O(2)^{iv}–V(3)–O(3)^{iv}	80.4(1)		
O(2)^{iv}–V(3)–O(4)	156.8(2)	O(2)^{iv}–V(3)–O(5)	101.5(2)		
O(3)^{ii}–V(3)–O(3)^{iii}	145.6(2)	O(3)^{ii,iii}–V(3)–O(3)^{iv}	76.5(1)		
O(3)^{ii,iii}–V(3)–O(4)	96.9(1)	O(3)^{ii,iii}–V(3)–O(5)	103.8(1)		
O(3)^{iv}–V(3)–O(4)	76.4(2)	O(3)^{iv}–V(3)–O(5)	178.2(2)		
O(4)–V(3)–O(5)	101.7(2)				
$V(4)O_6$ octahedron					
V(4)–O(4)^{iv}	1.927(4)	V(4)–O(6)	1.959(4)	V(4)–O(7)^{ii,iii}	1.858(2)
V(4)–O(8)	2.602(5)	V(4)–O(11)	1.601(5)		
O(4)^{iv}–V(4)–O(6)	154.9(2)	O(4)^{iv}–V(4)–O(7)^{ii,iii}	88.6(1)		
O(4)^{iv}–V(4)–O(8)	67.9(1)	O(4)^{iv}–V(4)–O(11)	103.3(2)		
O(6)–V(4)–O(7)^{ii,iii}	85.2(1)	O(6)–V(4)–O(8)	87.0(2)		
O(6)–V(4)–O(11)	101.8(2)	O(7)^{ii}–V(4)–O(7)^{iii}	150.8(3)		
O(7)^{ii,iii}–V(4)–O(8)	76.0(1)	O(7)^{ii,iii}–V(4)–O(11)	104.5(1)		
O(8)–V(4)–O(11)	171.2(2)				

Note. Symmetry codes: (i) $x + 1, 0, z$; (ii) $x + 1/2, 1/2, z$; (iii) $x + 1/2, -1/2, z$; (iv) $1 - x, 0, -z$.

temperatures above 300°C, and around 350°C $Ba_{1+x}V_6O_{16} \cdot nH_2O$ disappears in the product. In the hydrothermal system of $BaCl_2$–VO_2, where $Ba(NO_3)_2$ is substituted for $BaCl_2$, other barium vanadium bronzes, namely, green powders of δ-$Ba_xV_2O_5 \cdot nH_2O$ ($x \approx 0.15$) (16) or black

TABLE 5
Ba–O Bond Distances (Å) in BaO_9 Polyhedron

Ba–O(5)	2.877(4)	Ba–O(6)^{i,ii}	2.928(4)
Ba–O(7)	2.925(4)	Ba–O(8)^{i,ii}	2.951(4)
Ba–O(10)^{iii,iv}	2.952(4)	Ba–O(11)	2.845(5)

Note. Symmetry codes: (i) $x + 1, 0, z$; (ii) $x + 1/2, 1/2, z$; (iii) $x + 1/2, -1/2, z$; (iv) $1 - x, 0, -z$.

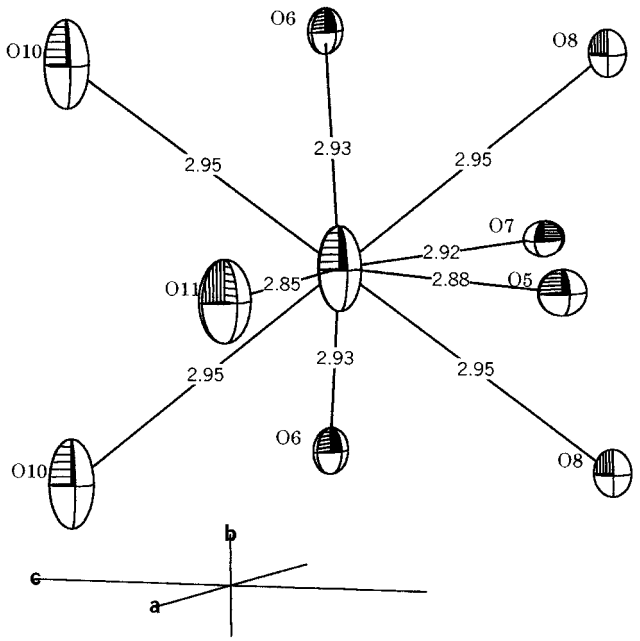

FIG. 3. ORTEP drawing for BaO_9 polyhedron.

crystals of BaV_3O_8 with more reduced states of V, are produced instead of $Ba_{1+x}V_8O_{21}$, indicating that NO_3^- ions play a significant role of oxidizing V^{IV} to V^{V}. Consequently, hydrothermal synthesis of $Ba_{1+x}V_8O_{21}$ requires a V^{IV}

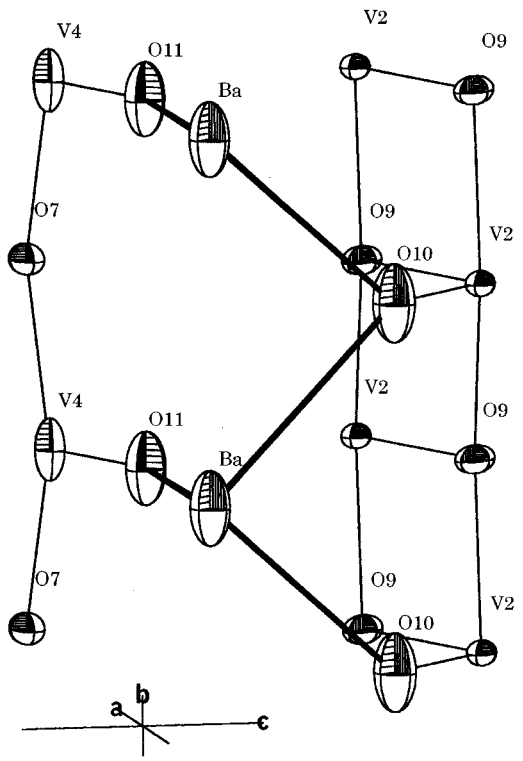

FIG. 4. Representation of atomic displacements in Ba–O–V bonding.

TABLE 6
Bond Valence Calculations for V Atoms of $Ba_{1+x}V_8O_{21}$

	V^{Va}	V^b
V(1)	4.99	4.85
V(2)	5.07	5.08
V(3)	5.06	4.93
V(4)	4.90	4.75

[a] Calculated by the equation in Ref. (14) for V^V–O.
[b] Calculated by the equation in Ref. (15) for V–O.

species of VO_2, an oxidizing agent of $Ba(NO_3)_2$ and higher reaction temperatures well above 300°C.

Since $Ba_{1+x}V_8O_{21}$ has partially occupied interstitial sites, reactivities such as ion exchange and Ba^{2+} ion incorporation are expected. As a result, no appreciable ion-exchange activity for alkali–metal ions was observed and no more Ba^{2+} ions were incorporated by treating in BaI_2 solution.

Barium Vanadium Bronzes and Related Compounds

As described in the preceding section, barium vanadium bronzes are apt to have layered types. Only the tunnel-type barium vanadium bronze would be β-$Ba_{0.17}V_2O_5$ reported by Bouloux *et al.* (8), which seems to be a barium analogue of the well-known tunnel-type β-phase vanadium bronze like β-$Na_{0.33}V_2O_5$ (17). But its structure has not been determined and only cell dimensions are given. Consequently, the present bronze $Ba_{1+x}V_8O_{21}$ presents the first example of a tunnel-type barium vanadium bronze whose structure has been fully characterized.

As for compounds related to $Ba_{1+x}V_8O_{21}$, first, it should be noted that Garbe and Range (18) reported, in an abstract of proceedings, on the structure of $Rb_4V_{16}O_{42}$ having the monoclinic system $C2/m$ with $a = 15.182$, $b = 3.65$, $c = 14.912$ Å, and $\beta = 90.13°$. They showed an illustration of a V–O octahedral framework of $Rb_4V_{16}O_{42}$ structure, which bears a strong resemblance to that of $Ba_{1+x}V_8O_{21}$. However, the structural details such as atomic coordinates were not given in the abstract and our literature survey failed to locate their paper of full structural data. It is considered, based on the limited information, that $Rb_4V_{16}O_{42}$ is probably a Rb analogue of $Ba_{1+x}V_8O_{21}$, namely, a stoichiometric compound of V^V with fully occupied tunnel sites by the Rb atom. Second, Fotiev *et al.* (9) reported that the compound BaV_8O_{21-x} was obtained by rapid cooling of the melt and Bouloux *et al.* (8) confirmed its existence in the BaO–V_2O_5–VO_2 phase diagram. Its structure has remained unknown but the powder X-ray diffraction pattern of BaV_8O_{21-x} is quite different from that of the present $Ba_{1+x}V_8O_{21}$, indicating both compounds have no relation to each other.

ACKNOWLEDGMENTS

The authors are grateful to Drs. K. Kato and Y. Kanke for their valuable discussion on the crystal structure.

REFERENCES

1. M. S. Whittingham, R. Chen, T. Chirayil, and P. Zavalij, *Solid State Ionics* **97,** 227 (1997).
2. Y. Ueda, *Chem. Mater.* **10,** 2653 (1998).
3. Y. Oka, T. Yao, and N. Yamamoto, *J. Solid State Chem.* **117,** 407 (1995).
4. Y. Oka, T. Yao, and N. Yamamoto, *J. Solid State Chem.* **140,** 219 (1998).
5. X. Wang, L. Liu, R. Bontchev, and A. J. Jacobson, *Chem. Commun.* 1009 (1998).
6. A. D. Wadsley, *Acta Crystallogr.* **10,** 261 (1957).
7. Y. Oka, O. Tamada, T. Yao, and N. Yamamoto, *J. Solid State Chem.* **114,** 359 (1995).
8. J. C. Bouloux, J. Galy, and P. Hagenmuller, *Rev. Chim. Miner.* **11,** 48 (1974).
9. A. A. Fotiev, V. V. Makarov, V. L. Volkov, and L. L. Surat, *Russ. J. Inorg. Chem.* **14,** 144 (1969).
10. Y. Oka, T. Yao, and N. Yamamoto, *J. Solid State Chem.* **86,** 116 (1990).
11. T. Yao, Y. Oka, and N. Yamamoto, *Inorg. Chim. Acta* **238,** 165 (1995).
12. "SDP for Windows." B. A. Frenz and Associates, Inc., 1997.
13. "teXsan for Windows: Crystal Structure Analysis Package." Molecular Structure Corp., The Woodlands, TX, 1997.
14. I. D. Brown and K. K. Wu, *Acta Crystallogr. Sect. B* **32,** 1957 (1976).
15. K. Waltersson, "Chem. Commun. Univ. of Stockholm," no. 7, 1976.
16. Y. Oka, T. Yao, and N. Yamamoto, unpublished work.
17. A. D. Wadsley, *Acta Crystallogr.* **8,** 695 (1955).
18. C. Garbe and K. J. Range, *Z. Kristallogr.* **156,** 43 (1981).